Numerical Study on the Gas-liquid Transportation in μDMFC Anode Flow Channel with Different Wettabilities Design

M M Li*, Z Li, J Geng and J H Shi

Nanjing University of Aeronautics and Astronautics, Nanjing, 210016, China

Corresponding author and e-mail: M M Li, limiaomiao@nuaa.edu.cn

Abstract. The gas-liquid flow in anode flow channel of micro direct methanol fuel cell (μDMFC) is simulated using the VOF method. The effect of channel sidewalls wettability on the gas-liquid transportation is investigated. Results indicate that improving hydrophilicity of the sidewall could promote removal of CO_2 bubbles when the wettability of the sidewall keeps the same everywhere. When the wettability of the sidewall changes with height, the hydrophilic/neutral combinations have the highest pressure drop, but the hydrophilic/hydrophobic combinations have the lowest gas fraction in the channel. Comparing the two aspects, a conclusion was drawn that sidewalls with hydrophobic upside and hydrophilic downside facilitate the CO_2 bubble removal and liquid transporting to GDL.

1. Introduction

In recent years, micro direct methanol fuel cell (μDMFC) based on MEMS technology is considered as a promising power source candidate for portable electronic equipments due to its advantages such as low temperature operation, high energy conversion, simple structure and convenience of refilling the liquid fuel [1-3].

The electrochemical reaction taking place in the μDMFC anode is described as follows:

$$CH_3OH + H_2O \xrightarrow{Pt-Ru} CO_2 + 6H^+ + 6e^- \quad (1)$$

As shown in Figure 1, when the μDMFC is in operation, carbon dioxide (CO_2) bubbles are generated on the surface of the anode catalyst layer because of the oxidation of the carbon in the methanol. The reaction-produced CO_2 bubbles emerge from the micro-pores of the gas diffusion layer (GDL) and transport into the sub-micrometer anode channel, and then move along the flow channel and out of the fuel cell, which lead to a liquid-gas two-phase flow in the anode flow field of μDMFC. The CO_2 bubbles could block the channel if not removed efficiently. In that case, not only less fuel reaches the catalyst layer but also the reaction sites are occupied by the bubbles, resulting in a decline of the performance of the μDMFC. Hence the effective removal of CO_2 in the anode micro channels plays - a critical role in the performance of the μDMFC.

Recently, researchers focus their attention on optimizing the channel by changing the wettability of the surfaces. Zhang et al. [4] investigated the effect of the wettabilities of the anode GDLs on CO_2 removal on these anode GDLs, and the visualizations of CO_2 gas bubbles dynamics on the anodes shows that uniform CO_2 gas bubbles with smaller size formed on hydrophilic anode GDLs, and

Li, M., Li, Z., Geng, J. and Shi, J.
Numerical Study on the Gas-liquid Transportation in μDMFC Anode Flow Channel with Different Wettabilities Design.
In *Proceedings of the International Workshop on Materials, Chemistry and Engineering (IWMCE 2018)*, pages 207-214
ISBN: 978-989-758-346-9

bubbles with larger size are not uniform over the hydrophobic anode GDLs. Ke et al. [5] studied the effects of hydrophilic/hydrophobic properties on liquid distribution and gas behavior by commercial

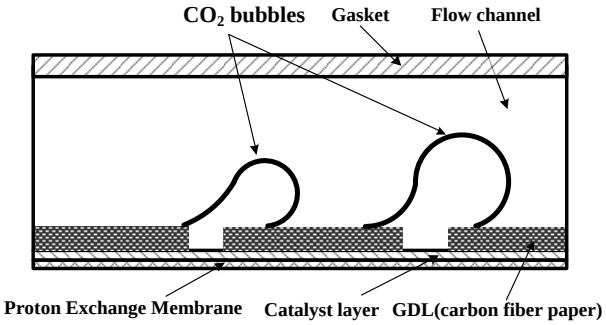

Figure 1. Schematic of the anode flow field of Mdmfc.

software Fluent. It was found that an anode channel with hydrophilic channel side-wall and hydrophobic GDL surface avoided gas accumulation on the GDL surface, and facilitated the gas discharging and liquid transporting to GDL. Hutzenlaub et al. [6] investigated the effect of both channel wall and diffusion layer wettability by observing two-phase flow from the side at different mean velocities of the fuel supply in 2011. By comparing hydrophobic and hydrophilic flow channel surfaces experimentally, they found that the hydrophilic flow channel leads to a minimum pressure drop along the channel. Comprehensive studies focusing on the effect of surface wettability properties on water droplet movement in PEM fuel cells has been conducted numerically with VOF method by Mondal et al. [7] and Zhu et al. [8].

In this paper, the effect of wettability of sidewalls on the gas-liquid transportation in μDMFC anode flow channel is investigated numerically by using the VOF method. The numerical model and the VOF method are briefly explained, and followed by description on the specific information of simulation performed. The simulation results for different wettabilities of sidewalls are compared and several useful conclusions are obtained.

2. Numerical method and numerical model

2.1. Numerical method and numerical model

Unsteady state and isothermal laminar flow conditions are assumed to prevail for both methanol flow and CO_2 bubble motion inside the microchannel, since the flow Reynolds number is far less than 2000. The three-dimensional numerical model was implemented by using the commercial CFD package, FLUENT, and the VOF method [9].

In the VOF technique, a single set of momentum equations is shared by both fluid phases, and the interface between phases is tracked for each computational cell throughout the domain by computing the volume fraction for the fluid k:

$$C_k(x,y,z,t)=\begin{cases}0 & (\text{outside } k\text{th fluid})\\ 1 & (\text{inside } k\text{th fluid})\\ 0\sim 1 & (\text{at the } k\text{th fluid interface})\end{cases} \quad (2)$$

Where C_k is the volume fraction function of kth fluid. For all the fluids, the sum of the volume fraction function is equal to 1.

$$\sum_{k=1}^{n} C_k = 1 \tag{3}$$

The volume fraction function C_k is governed by the volume fraction equation [9] which is solved in every computational cell.

$$\frac{\partial}{\partial t}(C_k \rho_k) + \nabla \cdot (C_k \rho_k \vec{u}_k) = 0 \tag{4}$$

Then, the two-phase fluid flows in the microchannel are modeled by the Navier-Stokes equation which depends on the volume fractions of all phases through the fluid properties ρ and μ.

$$\frac{\partial}{\partial t}(\rho \vec{u}) + \nabla \cdot (\rho \vec{u}\vec{u}) = -\nabla p + \nabla \cdot [\mu(\nabla \vec{u} + \nabla \vec{u}^T)] + \rho \vec{g} + \vec{F} \tag{5}$$

where p is the static pressure, $\vec{F}$ is a momentum source term related to surface tension, ρ and μ are the volume averaged density and dynamic viscosity. These are computed to account for the variable volume fractions for the two-phase air-water system considered here:

$$\rho = \rho_1 + C_2(\rho_2 - \rho_1) \tag{6}$$

$$\mu = \mu_1 + C_2(\mu_2 - \mu_1) \tag{7}$$

where 1 and 2 represent air and water, respectively

Surface tension is accounted for by using the continuum surface force (CSF) model, and is expressed in terms of the pressure jump across the interface, which depends on the surface tension coefficient, and is implemented in the momentum equation as a body force $\vec{F}$:

$$\Delta p = \sigma(\frac{1}{R_1} + \frac{1}{R_2}) \tag{8}$$

$$\vec{F}_{vol} = \sigma \kappa_k \frac{\rho \nabla C_k}{(1/2)(\rho_1 + \rho_2)} \tag{9}$$

where Δp is the pressure drop across the surface, σ the surface tension coefficient, R_1 and R_2 are the surface curvatures as measured by two radii in orthogonal directions. The curvature κk is computed from local gradients in the surface normal to the interface,

$$\kappa_k = \nabla \cdot (\frac{\vec{n}}{|\vec{n}|}) \tag{10}$$

and the surface normal $\vec{n}$ is defined as the gradient of C_k, the volume fraction of the kth phase.

$$\vec{n} = \nabla C_k \tag{11}$$

2.2. Numerical model

Figure 2 and Figure 3 shows the computational domain representing a part of the microchannel. Figure 2 is single-layer flow channel, Figure 3 is double-layered flow channel.Base case conditions in this study correspond to a microchannel with 400μm×400μm square cross section and 12000μm length. These dimensions are representative of flow channels used in μDMFC. A structured orthogonal computational mesh with 30,000 cells is used for the baseline case. The grid dependency was tested by increasing and decreasing the number of grid nodes by 20% for the baseline case, and

similar CO_2 bubble transport processes were obtained with all three grids. Therefore, the mesh used in the simulation is considered adequately. Preliminary simulations were performed with time steps of 10-5, 10-6 and 10-7 s, and all simulations were consequently performed using the time step of 10-6 s.

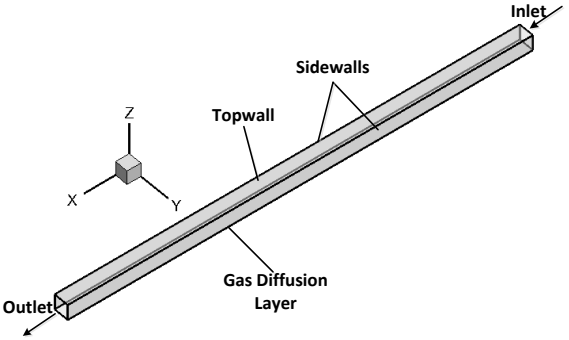

Figure 2. Computation domain of μDMFC anode single-layer flow channel.

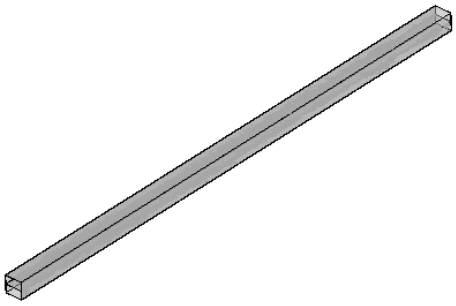

Figure 3. Computation domain of μDMFC anode double-layer flow channel.

3. Boundary and Initial Conditions

All VOF simulations were performed in the current study by employing uniform velocity profiles for the incoming gas and methanol solution in the channel, as shown in Figure 2. A convective outflow condition is used at outlet. No-slip boundary condition is imposed on walls of the channel. Constant surface tension and static contact angle are specified on the walls as a boundary condition.

For all simulations, a CO_2 inlet velocity of 0.1m/s is used and the liquid inlet velocity is set to 0.2m/s. The static contact angle of the GDL and topwall is set to 30° for all cases. However, the contact angle of all sidewalls of the microchannel is set to different values for different cases, representing different wettabilities of sidewalls.

The effect of wettability of sidewalls is studied from two aspects. Firstly, sidewalls have a single wettability in each case, that is, the contact angle keeps the same on the sidewalls. The two-phase flow in the channel was simulated under different wetting conditions. All the conditions are shown in Table 1, in which contact angle of 30° and 60° correspond to hydrophilic sidewalls and contact angle of 120° and 150° correspond to hydrophobic sidewalls.

Table 1. Computing conditions of single wettability.

Conditions	1	2	3	4	5
Contact angle of sidewalls (°)	30	60	90	120	150

Secondly, a double-layer channel with wettabilities of sidewalls changing with height is introduced as shown in Figure 3, the channel is divided to two parts with different wettability of sidewalls. Simulations were performed under six conditions, representing six combinations including hydrophilic/neutral (1), hydrophilic/hydrophobic (2), neutral/hydrophobic (3), neutral/hydrophilic (4), hydrophobic/hydrophilic (5), and hydrophobic/neutral(6). All the conditions are shown in Table 2.

Table 2. Computing conditions of single wettability.

Conditions	1	2	3	4	5	6
Contact angle of upside(°)	30	30	90	90	150	150

Contact angle of downside (°)	90	150	30	150	30	90

4. Results and discussion

Firstly, Figure 4. shows the changing curves of pressure drops of the gas-liquid flow between the inlet and outlet of the channel with different wettabilities. By data processing, Figure 5 gives comparison of average pressure drops for the cases with different wettabilities. Different wettablities of the sidewalls give significant differences in pressure drop of the flow in the channel from Figure 4 and Figure 5. Sidewall with contact angle of 30° corresponds to the highest average pressure drop, while sidewall with contact angle of 150° corresponds to the lowest average pressure drop. It could be found that the more hydrophilic sidewalls cause the higher pressure drop, which leads the faster bubble removal

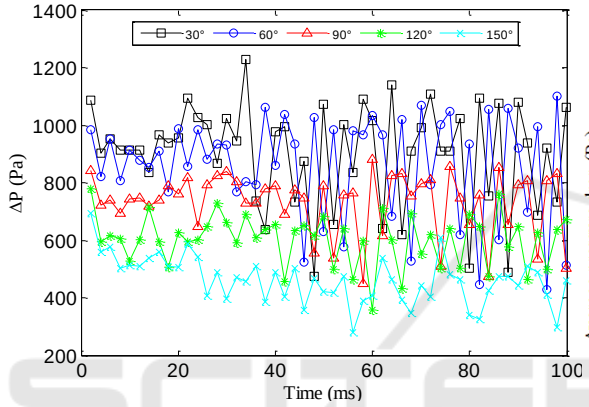

Figure 4. Pressure drops of the gas-liquid flow in channel with different wettabilities.

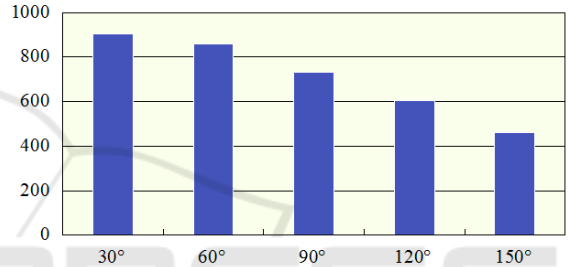

Figure 5. Columnar section of average pressure drops of the gas-liquid flow in channel with different wettabilities.

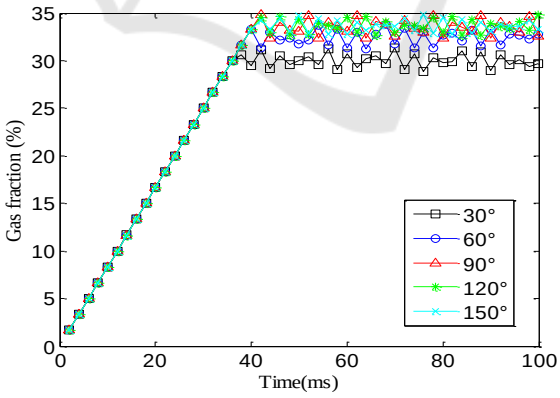

Figure 6. Gas fraction of the channels with different wettabilities.

Figure 6 gives comparison of gas fraction for the cases with different wettabilities. It could be distinguished that sidewall with contact angle of 30° has the lowest gas fraction of the channel. According to the above results, it could be concluded that improving hydrophilicity of the sidewall would promote removal of CO_2 bubbles.

Secondly, two-phase flow in a double-layer channel with wettabilities of sidewalls changing with height is simulated. Figure 7 shows the evolving processes of pressure drops of the gas-liquid flow

between the inlet and outlet of the channel with different wettability combinations. Since the curves are not very intuitive, average pressure drops are obtained by data processing, as shown in Figure 8. The exchange of the wettability combination order has little impact on the average pressure drop, e.g., the 30°-90° combination corresponds to the same average pressure drop with the 90°-30° combination. From Figure 8, we also find that a more hydrophilic sidewall on average results in a higher pressure drop between the inlet and outlet of the channel, which is, to some extent, similar with the conclusion we obtained from the above point; That is Figure 8 shows the average pressure drop of the gas-liquid flow in the flow channel with the difference of the contact angle between the upper and lower layers of the double-layered flow channel. The average value of the contact angle of the sidewall and the single-layer flow channel has the same variation trend. The average pressure drops slightly lower.

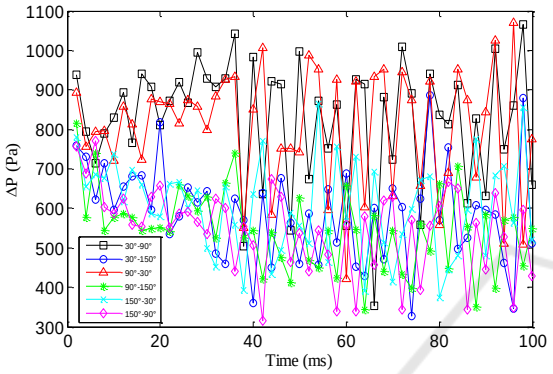

Figure 7. Pressure drops of the gas-liquid flow in channel with different wettability combinations.

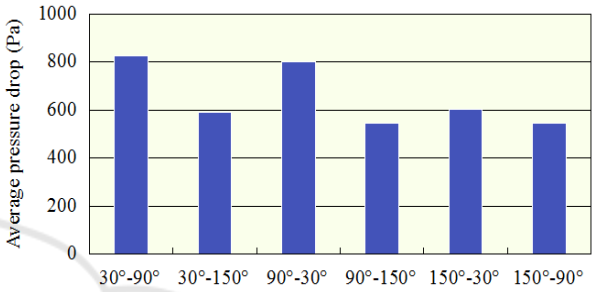

Figure 8. Columnar section of average pressure drops of the gas-liquid flow in channel with different wettability combinations.

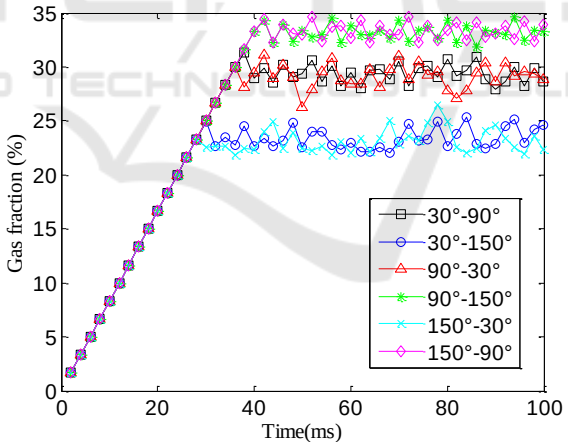

Figure 9. Gas fraction of the channels with different wettability combinations.

Figure 9 gives comparison of gas fraction for the cases with different wettability combinations. It could be found that the gas fraction is lowest when the sidewall is combined with hydrophilic and hydrophobic parts. CO_2 bubbles could be removed from the channel in the shortest time as well. However, when the sidewall is combined with neutral and hydrophobic parts, the gas fraction is highest and the removal of bubbles costs the longest time. Similarly, the exchange of the wettability combination order doesn't change the gas fraction in general. Dissimilarly, the 30°-150° combination and 150°-30° combination have the lowest gas fraction in the channel, which is different with the wettability combinations with the highest pressure drop, i.e., the 30°-90° combination and the 90°-30° combination.

Figure 10, Figure 11 and Figure 12 show the gas-liquid flow in the channel with different wettability combinations. Because hydrophilic sidewalls have an effect of repulsion on the bubbles but absorption on the liquid, bubbles tends to contact with the less hydrophilic sidewalls. It gives an explanation for the phenomenon that the gas-liquid flow in the channel tends to be layered when the sidewall is combined with hydrophilic and hydrophobic parts. As shown in Figure 11, methanol solution mainly exists within the scope of the altitude where the hydrophilic sidewalls exist, while bubbles mainly flow within the scope of the altitude where the hydrophobic sidewalls exist. It partly explains why the combination of hydrophilic and hydrophobic leads to the lowest gas fraction in the channel.

In order to find out the best wettability scheme from all the schemes including single wettabilities and wettability combinations, Figure 13 gives comparison of gas fraction for the cases which promote CO_2 bubble's removal in the two aspects respectively. It is distinguished that the gas fraction of the gas-liquid flow is lower when the sidewall is combined with hydrophilic and hydrophobic parts than that when the sidewall is hydrophilic only. So the combination of hydrophilic and hydrophobic will facilitate the gas-liquid transportation in the channel. According to Figure 11, bubbles mainly gather in the upper half of the channel when upper part of the sidewall is hydrophilic and lower part is hydrophobic, which promotes methanol transportation to GDL. Therefore, sidewalls with hydrophobic upside and hydrophilic downside do good to the improvement of the performance of μDMFC.

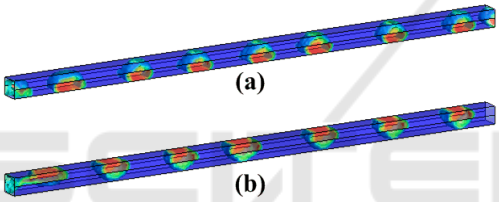

Figure 10. Gas-liquid flow in the channel combined with hydrophilic and neutral sidewalls (a) hydrophilic upside and neutral downside (b) neutral upside and hydrophilic downside.

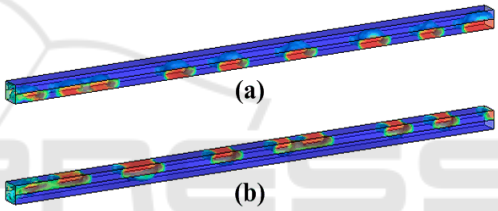

Figure 11. Gas-liquid flow in the channel combined with hydrophilic and hydrophobic sidewalls(a) hydrophilic upside and hydrophobic downside (b) hydrophobic upside and hydrophilic downside.

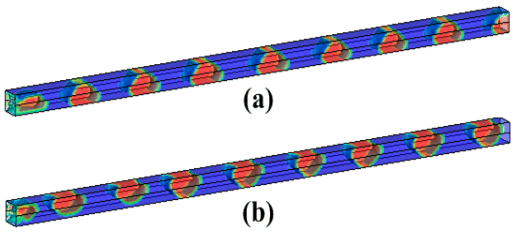

Figure 12. Gas-liquid flow in the channel combined with neutral and hydrophobic sidewalls(a) hydrophilic upside and hydrophobic downside (b) hydrophobic upside and

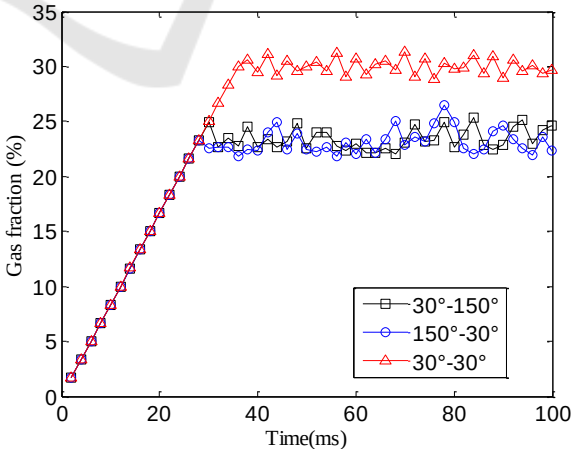

Figure 13. Gas fraction of the channels with hydrophilic sidewalls and hydrophilic/hydrophobic combined sidewalls.

hydrophilic downside.

5. Conclusions

The effect of wettability of sidewalls on the gas-liquid transportation in μDMFC anode flow channel is investigated numerically using the VOF method. The simulation results show that the wettability of sidewalls of the microchannel have a strong impact on the removal of CO_2 bubbles. When the wettability of the sidewall keeps the same everywhere, improving hydrophilicity of the sidewall could promote removal of CO_2 bubbles. When the wettability of the sidewall changes with height, the 30^o-90^o combination and the 90^o-30^o combination have the highest pressure drop, but the 30^o-150^o combination and 150^o-30^o combination have the lowest gas fraction in the channel. Comparing the two aspects, a conclusion was drawn that sidewalls with hydrophobic upside and hydrophilic downside facilitate the CO_2 bubble's removal and liquid transporting to GDL.

Acknowledgement

Authors are pleased to acknowledge the financial support provided by National Natural Science Foundation of China (Grants No 51505215) and the Natural Science Foundation of Jiangsu Province (Grants No BK20130804).

References

[1] Kamarudin S K, Achmad F and Daud W R W 2009 Overview on the application of direct methanol fuel cell (DMFC) for portable electronic devices *International Journal of Hydrogen Energy* **34(16)** 6902-6916

[2] Achmad F, Kamarudin S K, Daud W R W and et al 2011 Passive direct methanol fuel cells for portable electronic devices *Applied Energy* **88(5)** 1681-1689

[3] Thampan T, Shah D, Cook C and et al 2014 Development and evaluation of portable and wearable fuel cells for soldier use *Journal of Power Sources* **259** 276-281

[4] Zhang J, Yin G P, Lai Q Z and et al 2007 The influence of anode gas diffusion layer on the performance of low-temperature DMFC *J. Journal of power sources* **168(2)** 453-458

[5] Ke X, Yao K and Wang L 2008 Simulation of effects of hydrophilic properties of channel walls on the characteristics of gas-liquid two-phase flow in anode channel of DMFC *Chemical Industry and Engineering Progress* **27(2)** 265

[6] Hutzenlaub T, Paust N, Zengerle R and et al 2011 The effect of wetting properties on bubble dynamics and fuel distribution in the flow field of direct methanol fuel cells *Journal of Power Sources* **196** 8048–8056

[7] Mondal B, Jiao K and Li X 2011 Three-dimensional simulation of water droplet movement in PEM fuel cell flow channels with hydrophilic surfaces *J. International Journal of Energy Research* **35(13)** 1200-1212

[8] Zhu X, Sui P C, Djilali N and et al 2011 Dynamics of Emerging Water Droplet Subjected to Sidewall with Different Wettabilities in a Fuel Cell Cathode Channel *Fuel Cells* **11(3)** 404-412

[9] ANSYS FLUENT User's Guide Version 14.0 ANSYS Inc. 2011 Canonsburg PA